Inorganic Chemistry

Article

pubs.acs.org/IC

# $LiGaGe_2Se_6$: A New IR Nonlinear Optical Material with Low Melting Point

Dajiang Mei,[†,‡,§] Wenlong Yin,[†,‡,§] Kai Feng,[†,‡,§] Zheshuai Lin,[†,‡] Lei Bai,[†,‡] Jiyong Yao,*[,†,‡] and Yicheng Wu[†,‡]

[†]Center for Crystal Research and Development, Technical Institute of Physics and Chemistry, Chinese Academy of Sciences, Beijing 100190, People's Republic of China

[‡]Key Laboratory of Functional Crystals and Laser Technology, Technical Institute of Physics and Chemistry, Chinese Academy of Sciences, Beijing 100190, People's Republic of China

[§]Graduate University of the Chinese Academy of Sciences, Beijing 100049, People's Republic of China

Supporting Information

**ABSTRACT:** The new compound $LiGaGe_2Se_6$ has been synthesized. It crystallizes in the orthorhombic space group *Fdd*2 with $a$ = 12.501(3) Å, $b$ = 23.683(5) Å, $c$ = 7.1196(14) Å, and $Z$ = 8. The structure is a three-dimensional framework composed of corner-sharing $LiSe_4$, $GaSe_4$, and $GeSe_4$ tetrahedra. The compound exhibits a powder second harmonic generation signal at 2 $\mu$m that is about half that of the benchmark material $AgGaSe_2$ and possesses a wide band gap of about 2.64(2) eV. $LiGaGe_2Se_6$ melts congruently at a rather low temperature of 710 °C, which indicates that bulk crystals can be obtained by the Bridgman−Stockbarger technique. According to a first-principles calculation, there is strong hybridization of the 4*s* and 4*p* orbitals of Ga, Ge, and Se around the Fermi level. The calculated birefractive index is $\Delta n$ = 0.04 for $\lambda \geq 1$ $\mu$m, and the calculated major SHG tensor elements are $d_{15}$ = 18.6 pm/V and $d_{33}$ = 12.8 pm/V. This new material is promising for application in IR nonlinear optics.

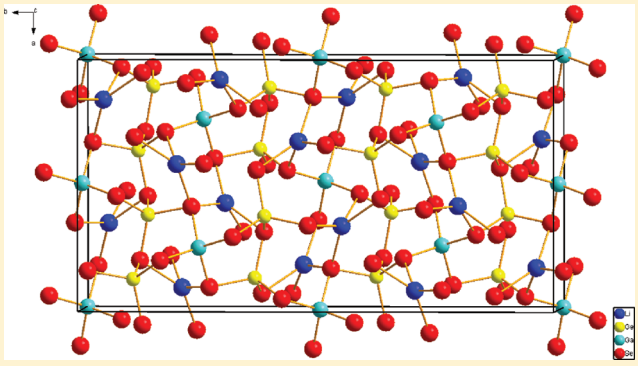

## INTRODUCTION

Many important civil and military applications including atmospheric monitoring, laser radar, laser guidance, and laser intrusion have been found for high average-power tunable midfar IR lasers in the range of 3−20 $\mu$m. An important method to convert existing laser sources to midfar IR wavelengths is frequency conversion with nonlinear optical (NLO) crystals. For decades, the $AgGaQ_2$ (Q = S, Se)[1,2] and $ZnGeP_2$[3] crystals have been the benchmark practically used IR NLO materials due to their large NLO coefficient and wide transparent range in the IR range. However, problems including nonphase-matching at 1 $\mu$m for $AgGaSe_2$, low laser damage threshold for $AgGaQ_2$ (Q = S, Se), and two photon absorption (TPA) of the conventional 1 (Nd:YAG) or 1.55 $\mu$m (Yb:YAG) laser pumping sources for $ZnGeP_2$ have seriously limited their applications.[4] Extensive research has been made to overcome these problems, leading to the findings of many new IR NLO materials.[5−13] The Li-containing IR NLO materials attract attention for their wide band gap, which is helpful to increase the laser damage threshold and avoid the TPA of the conventional 1 $\mu$m lasers. For example, the Li substitution for Ag in the $AgGaQ_2$ (Q = S, Se) has increased the band gap to 4.15 eV for $LiGaS_2$ and 3.34 eV for $LiGaSe_2$, which are much larger than those of 2.64 and 1.80 eV for the $AgGaS_2$ and $AgGaSe_2$, respectively.[14] However, a drawback of Li substitution is that it will reduce the NLO coefficients of the compounds presumably because of small polarization of the Li atom. For example, the NLO coefficient $d_{31}$ of $LiGaS_2$ and $LiGaSe_2$ are 5.8 and 10 pm/V, respectively,[14] which are significantly smaller than those of 12 pm/V for $AgGaS_2$ and 33 pm/V for $AgGaSe_2$.[2] Furthermore, the melting points of $LiGaS_2$ (1050 °C) and $LiGaSe_2$ (915 °C) are very high.[14] The Li elements could easily react with the silica ampule at the high crystal growth temperature. Although the problem can be alleviated by using carbon-coated silica ampule or graphite tube inside a silica tube, cracking of the silica tubes still often happens. One effective way to solve these two problems is to reduce the Li content in the compounds, which will increase the packing density of the microscopic NLO groups ($GaQ_4$ tetrahedra for example) and decrease the activity of Li to the silica tube. In addition, if the growth temperature could be decreased, the reactivity of Li will also be reduced. It has been shown that Ge doping in the $AgGaQ_2$ compounds can decrease the growth temperature significantly.[15,16] In view of all of the above discussion, the Li/Ga/Ge/Q (Q = S, Se, Te) systems are

**Received:** October 11, 2011
**Published:** December 21, 2011

   dx.doi.org/10.1021/ic202202j | *Inorg. Chem.* 2012, 51, 1035−1040

attractive, as shown by the discovery of the $Li_2Ga_2GeS_6$ compound in 2008.[8] However, the NLO coefficient and birefringence of $Li_2Ga_2GeS_6$ are still a bit small for application in the IR range according to our calculation. In this paper, we investigate the Li/Ge/Ga/Se system focusing on low Li content compounds. Our efforts led to the discovery of the low melting point, low Li content new IR NLO material $LiGaGe_2Se_6$, which exhibits a second harmonic generation (SHG) response at 2 $\mu$m that is approximately half that of the benchmark material $AgGaSe_2$ and melts congruently at the rather low temperature of 710 °C. The calculated birefringence is 0.04 for $\lambda \geq 1$ $\mu$m, which is similar with that of 0.05 in $LiGaSe_2$ and sufficiently large for achieving phase matching.[17] Here, we report the synthesis, crystal structure, and physical properties of $LiGaGe_2Se_6$.

## EXPERIMENTAL SECTION

**Solid-State Synthesis.** The binary staring materials, $Li_2Se$, $GeSe_2$, and $Ga_2Se_3$, were first synthesized by the stoichiometric reactions of the constituent elements in liquid $NH_3$ (for $Li_2Se$) or at high temperatures in sealed silica tubes (for $GeSe_2$ and $Ga_2Se_3$) using the following elements: Li (Sinopharm Chemical Reagent Co., Ltd., 98%), Ge (Sinopharm Chemical Reagent Co., Ltd., 99%), Se (Sinopharm Chemical Reagent Co., Ltd., 99%), and Ga (Sinopharm Chemical Reagent Co., Ltd., 99%). Then, polycrystalline samples of $LiGaGe_2Se_6$ were synthesized by solid-state reaction technique from stoichiometric amounts of $Li_2Se$ (0.093 g, 1 mmol), $GeSe_2$ (0.922 g, 4 mmol), and $Ga_2Se_3$ (0.376 g, 1 mmol). The starting materials were well mixed and loaded into a fused-silica tube under an Ar atmosphere in a glovebox and then sealed under $10^{-3}$ Pa atmosphere. The above sample was placed into a computer-controlled furnace, heated to 700 °C in 30 h, and kept at 700 °C for 72 h, and then, the furnace was turned off.

The X-ray powder diffraction pattern of the resultant powder sample was recorded at room temperature in the angular range of $2\theta$ = 10−70° with a scan step width of 0.02° and a fixed counting time of 1 s/step on an automated Bruker D8 X-ray diffractometer equipped with a diffracted monochromator set for Cu K$\alpha$ ($\lambda$ = 1.5418 Å) radiation. It was later found to be in agreement with the calculated pattern on the basis of the single crystal crystallographic data of $LiGaGe_2Se_6$ (Figure 1).

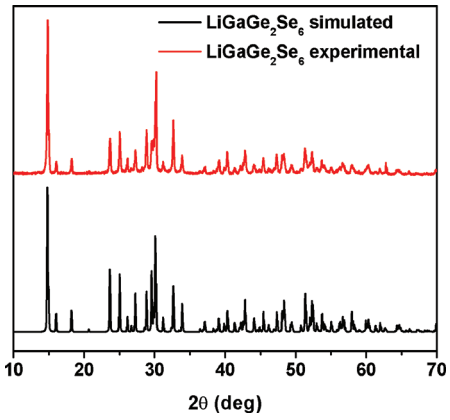


**Figure 1.** XRD pattern of bulk powder sample and the calculated pattern using the single-crystal crystallographic data.

**Single Crystal Growth.** The as-prepared yellow $LiGaGe_2Se_6$ powder was put into a fused-silica tube, which was then flame-sealed under high vacuum of $10^{-3}$ Pa and placed in a computer-controlled furnace. The sample was heated to 800 °C in 20 h, kept at 800 °C for 72 h, and then cooled at 2 °C/h to 300 °C, at which point the furnace was switched off. Many yellow block-shaped single crystals, subsequently determined as $LiGaGe_2Se_6$, were produced in the ampule. The crystals are air and moisture stable. ICP measurement on the crystals indicated that the molar ratio of Li:Ga:Se is close to 1:1:6 (Ge was not measured in ICP as it precipitated in the form of $H_4GeO_4$ in the acidic solution), and analysis of the crystals with EDX-equipped Hitachi S-3500 SEM showed the presence of Ge, Ga, and Se in the approximate molar ratio of 2:1:6 (Li is undetectable in EDX).

**Structure Determination.** A $LiGaGe_2Se_6$ single crystal with dimensions of 0.190 × 0.133 × 0.037 $mm^3$ was mounted on a glass fiber for single-crystal X-ray diffraction analysis. The measurement was performed on a Rigaku AFC10 diffractometer equipped with a graphite-monochromated K$\alpha$ ($\lambda$ = 0.71073 Å) radiation at 93 K. The Crystalclear software[18] was used for data extraction and integration, and the program XPREP[19] was used for face-indexed absorption corrections.

The structure was solved with the direct methods program SHELXS and refined with the least-squares program SHELXL of the SHELXTL.PC suite of programs.[19] Three Se atoms at general positions (Wyckoff position 16*b*) and three tetrahedral metal sites, M1 (Wyckoff position 16*b*), M2 (Wyckoff position 16*b*), and M3 (Wyckoff position 8*a*), were found. The small electron density at M1 site and the longer M1−Se distances make it easy to decide that Li takes this position. However, the Li atoms still exhibit a relatively large isotropical displacement parameter. Least squares refinement on its occupancy converges to 0.51(2) with a reasonable isotropical displacement parameter. The M2 (Wyckoff position 16*b*) and M3 (Wyckoff position 8*a*) possess high electronic density and should be occupied by Ga and Ge atoms. Although it is difficult for X-ray to differentiate between Ga and Ge, two facts give us some clue to the assignment of Ga and Ge positions in the structure. One is that the molar ratio of Ga:Ge is very close to 1:2 as determined by EDX measurement; the other is that the M2−Se distances [2.359(1)−2.371(1) Å] are slightly shorter than the M3−Se [2.378(1)−2.386(1) Å]. If Ge takes the M2 position and Ga takes the M3 position, the calculated bond valence sums (BVSs)[20,21] are 3.87 for Ge and 3.24 for Ga. In comparison, if Ga takes the M2 position and Ge takes the M3 position, the calculated BVSs are 3.69 for Ge and 3.39 for Ga. Thus, an ideal assignment of the atom types seems to be that Ga takes the Wyckoff 8*a* position and Ge takes the Wyckoff 16*b* position, although it may be safer to state that Ga and Ge are disordered at M2 and M3 positions with a ratio of Ga:Ge = 1:2. Considering the half occupancy of Li at the Wyckoff 16*b* position, there are eight Li atoms, eight Ga atoms, 16 Ge atoms, and 48 Se atoms in the unit cell, which give the chemical formula $LiGaGe_2Se_6$. This formula agrees well with ICP, EDX, and the X-ray diffraction data analysis on the crystals and satisfies the charge-balance requirement. The final refinement included anisotropic displacement parameters and a secondary extinction correction. The program STRUCTURE TIDY[22] was then employed to standardize the atomic coordinates. Additional experimental details are given in Table 1, and selected metrical data are given in Table 2. Further information may be found in the Supporting Information.

**Diffuse Reflectance Spectroscopy.** The diffuse reflectance spectrum of $LiGaGe_2Se_6$ was measured on a Cary 5000 UV−visible-NIR spectrophotometer with a diffuse reflectance accessory over the range of 250 (5 eV) to 2500 nm (0.50 eV).

**Thermal Analysis.** A Labsys TG-DTA16 (SETARAM) thermal analyzer was used to measure the differential scanning calorimetric (DSC) curve of $LiGaGe_2Se_6$. About 20 mg of $LiGaGe_2Se_6$ sample was loaded in a carbon-coated silica tube (5 mm o.d. × 3 mm i.d.) and subsequently sealed under high vacuum. The heating and the cooling rates were both 30 °C/min.

**SHG Measurement.** The optical SHG response of $LiGaGe_2Se_6$ was measured by means of the Kurtz−Perry method.[23] The fundamental light is the 2090 nm light generated with a Q-switched Ho:Tm:Cr:YAG laser. The particle size of the sieved sample is 80−100 $\mu$m. Microcrystalline $AgGaSe_2$ of similar particle size served as a reference.

**Theoretical Calculation.** Electronic structure calculation of $LiGaGe_2Se_6$ was performed using the plane-wave pseudopotential method[24] implemented in the CASTEP package,[25] which applies the


dx.doi.org/10.1021/ic202202j | Inorg. Chem. 2012, 51, 1035−1040

**Table 1. Crystal Data and Structure Refinement for $LiGaGe_2Se_6$**

| | $LiGaGe_2Se_6$ |
|---|---|
| fw | 695.6 |
| $T$ (°C) | −180 |
| $a$ (Å) | 12.501(3) |
| $b$ (Å) | 23.683(5) |
| $c$ (Å) | 7.1196(14) |
| $V$ (Å$^3$) | 2107.84(79) |
| space group | $Fdd2$ |
| $Z$ | 8 |
| $\rho_c$ (g/cm$^3$) | 4.384 |
| $\mu$ (cm$^{-1}$) | 288.55 |
| $R(F)^a$ | 0.0373 |
| $R_w(F_o^2)^b$ | 0.0689 |

$^aR(F) = \sum||F_o| - |F_c||/\sum|F_o|$ for $F_o^2 > 2\sigma(F_o^2)$. $^bR_w(F_o^2) = \{\sum[w(F_o^2 - F_c^2)^2]/\sum wF_o^4\}^{1/2}$ for all data. $w^{-1} = \sigma^2(F_o^2) + (zP)^2$, where $P = [\max(F_o^2, 0) + 2F_c^2]/3$; $z = 0.009$.

**Table 2. Selected Bond Lengths (Å) and Angles (deg) for $LiGaGe_2Se_6$**

| | | | |
|---|---|---|---|
| | $LiSe_4$ tetrahedron | | |
| Li−Se1 | 2.84(4) | Se2−Li−Se3 | 96.6(12) |
| Li−Se2 | 2.61(3) | Se2−Li−Se3 | 144.1(15) |
| Li−Se3 | 2.64(4) | Se3−Li−Se3 | 108.5(11) |
| Li−Se3 | 2.68(3) | Se2−Li−Se1 | 81.2(9) |
| | | Se3−Li−Se1 | 142.2(16) |
| | | Se3−Li−Se1 | 93.2(12) |
| | $GeSe_4$ tetrahedron | | |
| Ge−Se1 | 2.3710(12) | Se3−Ge−Se2 | 113.60(4) |
| Ge−Se2 | 2.3605(11) | Se3−Ge−Se1 | 107.49(4) |
| Ge−Se2 | 2.3713(12) | Se2−Ge−Se1 | 114.12(4) |
| Ge−Se3 | 2.3585(11) | Se3−Ge−Se2 | 106.65(4) |
| | | Se2−Ge−Se2 | 99.25(4) |
| | | Se1−Ge−Se2 | 115.54(4) |
| | $GaSe_4$ tetrahedron | | |
| Ga−Se1 × 2 | 2.3780(11) | Se1−Ga−Se1 | 105.82(6) |
| Ga−Se3 × 2 | 2.3863(11) | Se1−Ga−Se3 × 2 | 112.01(3) |
| | | Se1−Ga−Se3 × 2 | 104.33(3) |
| | | Se3−Ga−Se3 | 117.89(7) |

preconditioned conjugated gradient (CG) band-by-band method[26] to ensure a robust efficient search of the energy minimum of the electronic structure ground state. The geometric parameters and atomic positions of $LiGaGe_2Se_6$ directly come from the experimental determination. To consider the fractional occupancy of Li site in crystal, the virtual crystal approximation (VCA)[27] is used. It is because atomic sites in a crystal can be described in terms of a hybrid atom that consists of two or more element types. So, the VCA method allows us to model the half occupancy of the Li site by defining the "mixture" Li atom where half of the mixture is an atom of "nothing". The local density functional (LDA) with a high kinetic energy cutoff of 800 eV is adopted. The optimized normal-conserving pseudopotentials[28] in Kleinman−Bylander form[29] for Li, Ga, Ge, and Se allow us to use a small plane-wave basis set without compromising the accuracy required by our study. The electrons 1s orbital for lithium are treated as the core electrons. For gallium, the 3d, 4s, and 4p electrons are chosen as the valence electrons, and for selenium and germanium, they are 4s and 4p electrons. Monkhorst−Pack $k$-point meshes[30] with a density of (2 × 1 × 4) points in the Brillouin zone of the unit cell are chosen.

On the basis of the above electronic band structure, the virtual excitation processes under the influence of an incident radiation were simulated, and the refractive indices and SHG coefficients of $LiGaGe_2Se_6$ were obtained according to the formulas given in ref 31. It is well-known that the LDA energy band gap is usually smaller than the experimental value because of the discontinuity of exchange-correlation energy. So, in these calculations, scissors operators[32,33] are used to rigidly shift all of the conduction band to agree with the measured value of the band gap.

## RESULTS AND DISCUSSION

**Structure.** $LiGaGe_2Se_6$ belongs to the $AgGaGeS_4$ structure type and crystallizes in the noncentrosymmetric orthorhombic space group $Fdd2$ with cell parameters of $a$ = 12.501(3) Å, $b$ = 23.683(5) Å, $c$ = 7.1196(14) Å, and $Z$ = 8. As discussed in the Experimental Section, although it is difficult for X-ray to tell Ge from Ga, it is reasonable to state that the Wyckoff position 16$b$ and the Wyckoff position 8$a$ are largely, if not solely, occupied by Ge and Ga atoms, respectively, based on the BVSs calculation and the elemental analysis by EDX. The asymmetric unit contains one crystallographically independent Li atom at Wyckoff position 16$b$ with 50% occupancy, one independent Ga atom at Wyckoff position 8$a$, one independent Ge atom Wyckoff position 16$b$, and three independent Se atoms Wyckoff position 16$b$. The Li, Ga, and Ge atoms are all coordinated to a slightly distorted tetrahedron of four Se atoms. The crystal structure of $LiGaGe_2Se_6$ is shown in Figure 2. The $LiSe_4$, $GaSe_4$, and $GeSe_4$ tetrahedra are connected to each other via corner sharing to generate a three-dimensional framework. The Li−Se distances range from 2.64(3) to 2.83(3) Å, which are close to those of 2.68(2)−2.902(16) Å in $\beta$-$LiAsSe_2$.[34] The Ga−Se distances of 2.3783(10)−2.3872(10) Å are comparable to those of 2.3740(6)−2.4400(6) Å for Ga−Se in $K_2CuGa_3Se_6$,[35] and the Ge−Se distances of 2.3594(12)−2.3711(11) Å are in good agreement with those in $Ba_2GeSe_2Te_2$ (2.35 Å).[36] Because there are no Se−Se bonds in the structure, the oxidation states of 1+, 3+, 4+, and 2− can be assigned to Li, Ga, Ge, and Se, respectively.

**Experimental Band Gap.** On the basis of the UV−visible-NIR diffuse reflectance spectrum of $LiGaGe_2Se_6$ (Figure 3), A band gap of 2.64 (2) eV could be deduced by the straightforward extrapolation method,[37] which is larger than that of $AgGaSe_2$ (1.8 eV) but smaller than that of $LiGaSe_2$ (3.34 eV). A large band gap is helpful to increase the laser damage thresholds of IR NLO materials. Thus, $LiGaGe_2Se_6$ may possess a higher laser damage threshold than the benchmark material $AgGaSe_2$. Besides, the band gap may enable $LiGaGe_2Se_6$ to avoid the two-photon absorption problem of the conventional 1 (Nd:YAG) or 1.55 $\mu$m (Yb:YAG) lasers, which has severely limited the application of the benchmark IR NLO crystal $ZnGeP_2$.[4]

**Thermal Analysis.** As shown in Figure 4, $LiGaGe_2Se_6$ crystal melts congruently at a rather low temperature of 710 °C. The congruent-melting behavior is also confirmed by the successful growth of $LiGaGe_2Se_6$ single crystal from melted $LiGaGe_2Se_6$ pure powder. The congruent-melting behavior makes it feasible to use the Bridgman−Stockbarger technique to grow bulk $LiGaGe_2Se_6$ crystals, which are needed for a thorough evaluation and practical application in IR NLO optics. In comparison, the melting points are 1050 °C for $LiGaS_2$, 915 °C for $LiGaSe_2$, 998 °C for $AgGaS_2$, 1025 °C for $ZnGeP_2$, and 860 °C for $AgGaSe_2$. The rather low melting point of $LiGaGe_2Se_6$ and the low volatility of Se vs S and P will favor the crystal growth by the Bridgman−Stockbarger technique. Besides, the low-crystal growth temperature and the low Li content of $LiGaGe_2Se_6$ could also effectively reduce the


dx.doi.org/10.1021/ic202202j | Inorg. Chem. 2012, 51, 1035−1040

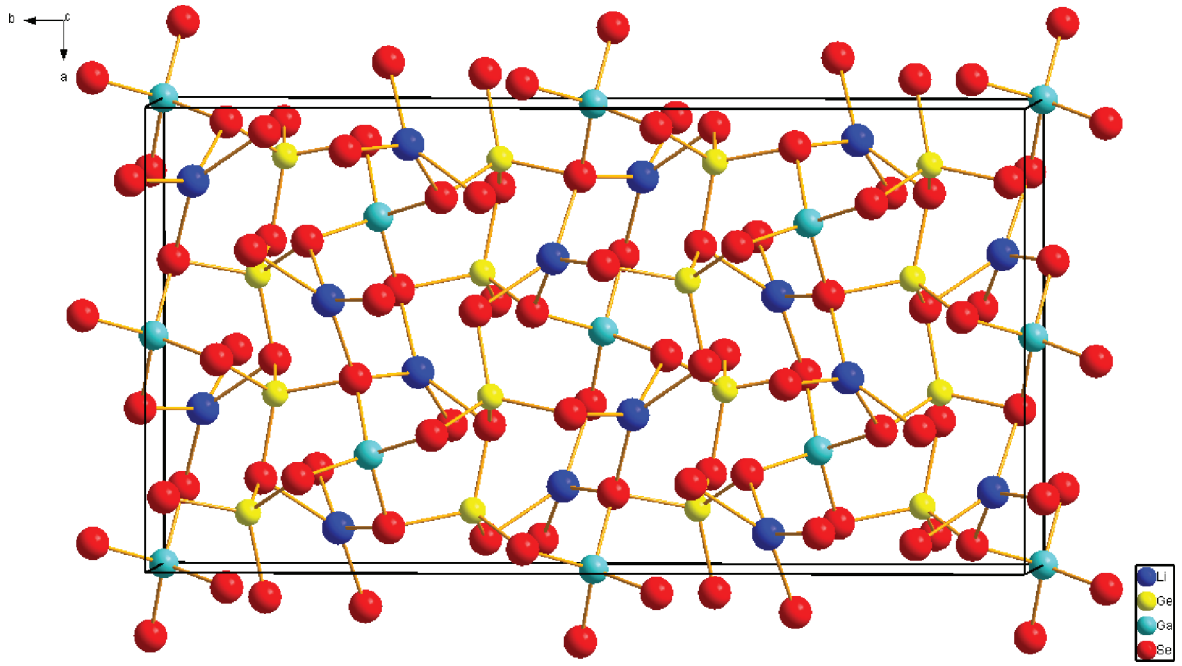


**Figure 2.** Unit cell of the $LiGaGe_2Se_6$ structure.

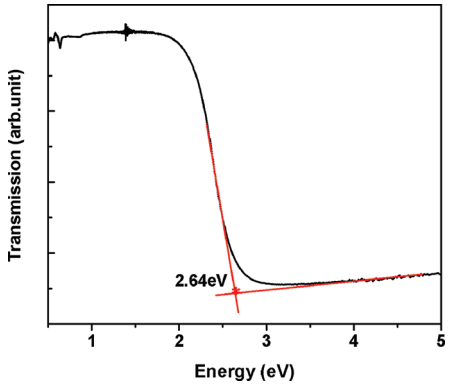


**Figure 3.** Diffuse reflectance spectrum of $LiGaGe_2Se_6$.

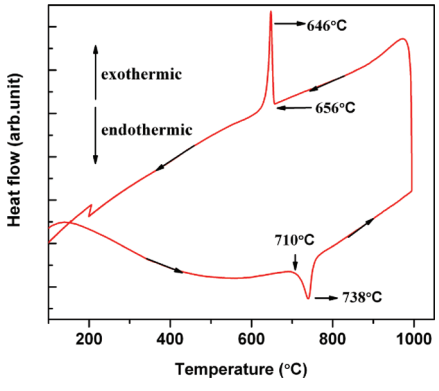


**Figure 4.** DSC curve of $LiGaGe_2Se_6$.

attacking of Li atom to the silica tube, which may provide an additional advantage for the crystal growth of $LiGaGe_2Se_6$.

**SHG Measurement.** The SHG signal intensity of $LiGaGe_2Se_6$ with the use of the 2090 nm laser as fundamental wavelength was about half that of $AgGaSe_2$ with similar particle size. Considering the large NLO effect of $AgGaSe_2$ ($d_{36}$ = 33 pm/V), the NLO response of $LiGaGe_2Se_6$ is sufficient for application in IR NLO optics, which is also consistent with the prediction of the theoretical calculations (see the Electronic Structure Calculation section).

**Electronic Structure Calculation.** As shown in Figure 5, the calculated direct band gap is 1.62 eV. It is well-known that the band gap calculated by LDA is usually smaller than the

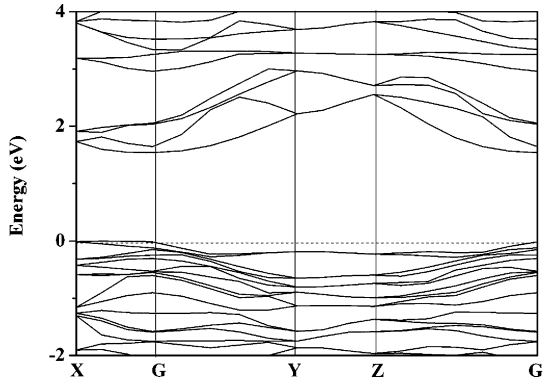


**Figure 5.** Band structure of $LiGaGe_2Se_6$ along the lines of high symmetry points in the Brillouin zone. The dash line indicates the VB maximum.

experimental data because of the discontinuity of exchange-correlation energy. In this work, an energy scissors operator (1.02 eV) is adopted to shift all of the conduction bands to agree with the measured value of the band gap (2.64 eV). Further calculations with other kinds of pseudopotentials show that the change of the results is not apparent.

With energy scissors operator adopted, Figure 6 gives the partial density of states (PDOS) projected on the constitutional atoms in $LiGaGe_2Se_6$, in which several electronic characteristics can be seen: (i) The Ga 3d orbitals are strongly localized in the deep region of the VB at about −15 eV, and these orbitals have no chemical bonding with other atoms. (ii) The VB from −14 to −11 eV are mainly composed by many of the Se 4s and


dx.doi.org/10.1021/ic202202j | Inorg. Chem. 2012, 51, 1035−1040

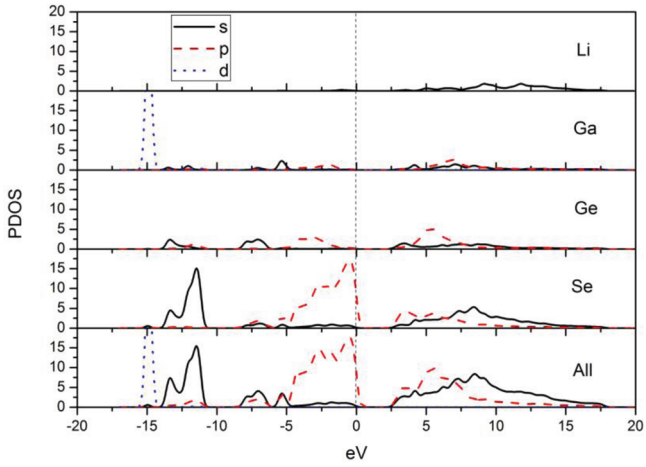


**Figure 6.** PDOS of $LiGaGe_2Se_6$. The solid, dot-dash, and dash lines are the s, p, and d orbitals, respectively. The broken vertical lines indicate the VB maximum.

some of Ge 4s, 4p orbitals, which have some contribution to the Ge−Se bonding. The upper of the valence states from −7 eV show some of hybridization between Ga 4s, Ge 4p, and Se 4p orbitals, indicating chemical bonds between the Ga, Ge, and Se atoms; obviously, the top of valence band maximum is dominated by Se 4p orbitals. (iii) The bottom of CB is mainly composed of the orbitals of Se and Ge atoms. Most of them are composed by 4s, 4p orbitals of Se and some of the Ge 4s orbitals, although the Ga 4s, 4p orbitals have a little contribution to the higher electronic levels of CB. Figure 7 shows the charge density contour on the Ga−Se−Ge plane in $LiGaGe_2Se_6$. Clearly, there are very high electronic density distributions (red color) in the Ga−Se and Ge−Se bonds, indicating their strong covalent chemical bonding. Meanwhile, the distribution of charge density around Li is low (blue color). This means that the Li cations are rather isolated; their covalent chemical bonding to the neighbor ions is very weak.

For the mentioned reasons, an energy scissors operator (1.02 eV) is adopted, which is in the good determination of the low-energy structures in the imaginary part of the dielectric functions. Table 3 lists the calculated refractive indices and birefringence at several radiation wavelengths. It is shown that the birefringence $\Delta n$ is about 0.04 as the wavelength $\lambda \geq 1$ $\mu$m, so $LiGaGe_2Se_6$ is phase-matchable for the SHG in the IR region. In addition, it overcomes problem of the nonphase matching at 1 $\mu$m for $AgGaSe_2$ ($\Delta n \sim 0.02$). Furthermore, we theoretically determined the SHG coefficients of $LiGaGe_2Se_6$ as follows: $d_{15}$ = 18.6 pm/V, $d_{24}$ = −9.3 pm/V, and $d_{33}$ = 12.8 pm/V. In comparison, the major SHG coefficient of $LiGaSe_2$ is $d_{31}$ = 10 pm/V. From the structure point of view, the molar percentages of Li are 1/10 and 1/4 in $LiGaGe_2Se_6$ and $LiGaSe_2$, respectively. Thus, the packing of the microscopic NLO functional groups, the $Ga(Ge)Se_4$ tetrahedra, is denser in $LiGaGe_2Se_6$ than in $LiGaSe_2$, which may be the reason why $LiGaGe_2Se_6$ has a higher SHG effect than $LiGaSe_2$.

## CONCLUSION

The new compound $LiGaGe_2Se_6$ has been synthesized for the first time. It adopts the $AgGaGeS_4$ structure type and crystallizes in the noncentrosymmetric space group *Fdd*2. The structure is a three-dimensional framework composed of $LiSe_4$, $GaSe_4$, and $GeSe_4$ tetrahedra via corner sharing. The material

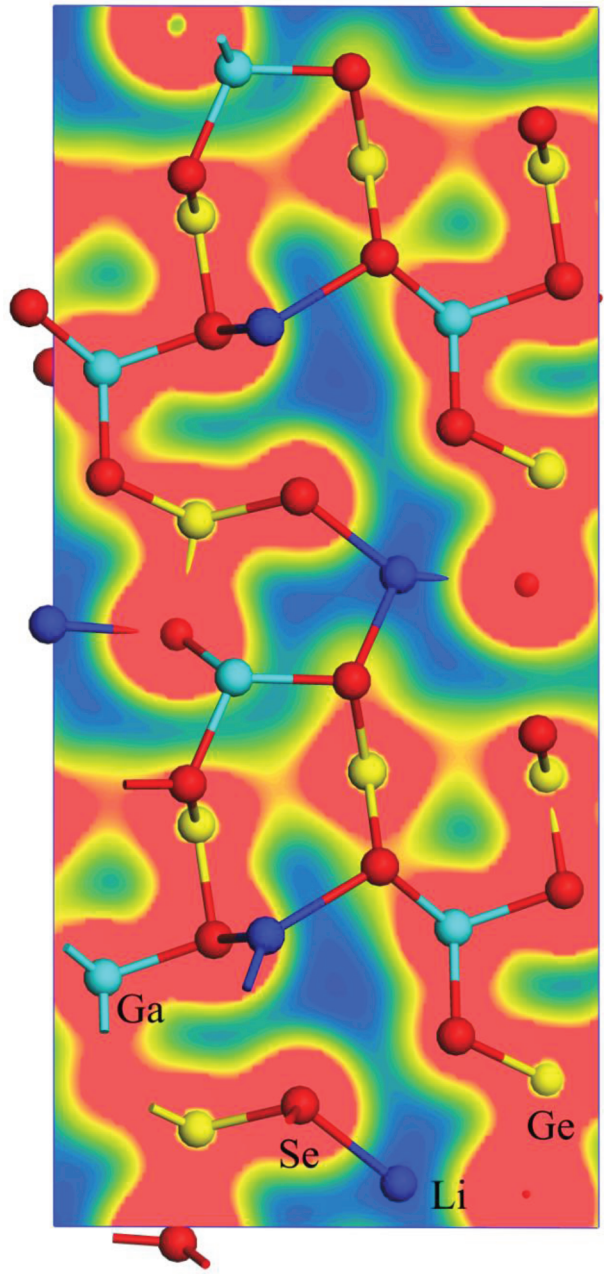


**Figure 7.** Charge density contour on the Ga−Se−Ge plane in $LiGaGe_2Se_6$. Li, Ga, Ge, and Se are represented by deep blue, light blue, yellow, and red balls, respectively.

**Table 3. Calculated Refractive Indices at Selected Wavelengths for $LiGaGe_2Se_6$**

| | 1.0 $\mu$m | 1.5 $\mu$m | 2.0 $\mu$m |
|---|---|---|---|
| $n_x$ | 2.64 | 2.60 | 2.59 |
| $n_y$ | 2.60 | 2.56 | 2.55 |
| $n_z$ | 2.61 | 2.57 | 2.56 |
| $\Delta n(n_x - n_y)$ | 0.04 | 0.04 | 0.04 |

exhibits a powder SHG response at 2 $\mu$m that is approximately half that of the benchmark material $AgGaSe_2$. $LiGaGe_2Se_6$ has a relatively large band gap (2.64 eV), which is very helpful for increasing the laser damage threshold and avoiding the TPA of conventional 1 $\mu$m lasers. It melts congruently at a rather low temperature of 710 °C. This congruent-melting behavior makes


dx.doi.org/10.1021/ic202202j | *Inorg. Chem.* 2012, 51, 1035−1040

the bulk crystal growth by the Bridgman−Stockbarger technique possible. Besides, the rather low melting point and low Li content of $LiGaGe_2Se_6$ will greatly reduce the attack of Li to the silica tube, which is good for crystal growth. The calculated birefractive index $\Delta n = 0.04$ as the wavelength $\lambda \geq 1$ $\mu$m, so $LiGaGe_2Se_6$ is phase matchable for the SHG in the IR region. In addition, it may be able to overcome problem of the nonphase matching at 1 $\mu$m for $AgGaSe_2$ ($\Delta n \sim 0.02$). The calculated major SHG tensor elements are $d_{15} = 18.6$ pm/V and $d_{33} = 12.8$ pm/V, which are obviously larger than that of the newly studied $LiGaSe_2$ ($d_{31} = 10$ pm/V). Our preliminary experimental and theoretical results indicated that $LiGaGe_2Se_6$ is promising IR NLO material for practical application. Further research is in progress.

## ■ ASSOCIATED CONTENT

### Supporting Information

Crystallographic file in CIF format for $LiGaGe_2Se_6$. This material is available free of charge via the Internet at http://pubs.acs.org.

## ■ AUTHOR INFORMATION


### Corresponding Author

*E-mail: jyao@mail.ipc.ac.cn.


## ■ ACKNOWLEDGMENTS

This research was supported by the National Basic Research Project of China (No. 2010CB630701) and National Natural Science Foundation of China (No. 51072203).

## ■ REFERENCES


(1) Chemla, D. S.; Kupecek, P. J.; Robertson, D. S.; Smith, R. C. *Opt. Commun.* **1971**, *3*, 29−31.
(2) Boyd, G. D.; Kasper, H. M.; McFee, J. H.; Storz, F. G. *IEEE J. Quantum Electron.* **1972**, *8*, 900−908.
(3) Boyd, G. D.; Buehler, E.; Storz, F. G. *Appl. Phys. Lett.* **1971**, *18*, 301−304.
(4) Schunemann, P. G. *AIP Conf. Proc.* **2007**, *916*, 541−559.
(5) Banerjee, S.; Malliakas, C. D.; Jang, J. I.; Ketterson, J. B.; Kanatzidis, M. G. *J. Am. Chem. Soc.* **2008**, *130*, 12270−12272.
(6) Chung, I.; Song, J. H.; Jang, J. I.; Freeman, A. J.; Ketterson, J. B.; Kanatzidis, M. G. *J. Am. Chem. Soc.* **2009**, *131*, 2647−2656.
(7) Guo, S. P.; Guo, G. C.; Wang, M. S.; Zou, J. P.; Xu, G.; Wang, G. J.; Long, X. F.; Huang, J. S. *Inorg. Chem.* **2009**, *48*, 7059−7065.
(8) Kim, Y.; Seo, I. S.; Martin, S. W.; Baek, J.; Halasyamani, P. S.; Arumugam, N.; Steinfink, H. *Chem. Mater.* **2008**, *20*, 6048−6052.
(9) Lin, X.; Zhang, G.; Ye, N. *Cryst. Growth. Des.* **2009**, *9*, 1186−1189.
(10) Yao, J.; Mei, D.; Bai, L.; Lin, Z.; Yin, W.; Fu, P.; Wu, Y. *Inorg. Chem.* **2010**, *49*, 9212−9216.
(11) Mei, D.; Yin, W.; Bai, L.; Lin, Z.; Yao, J.; Fu, P.; Wu, Y. *Dalton. Trans.* **2011**, *40*, 3610−3615.
(12) Chen, M.-C.; Li, L.-H.; Chen, Y.-B.; Chen, L. *J. Am. Chem. Soc.* **2011**, *133*, 4617−4624.
(13) Geng, L.; Cheng, W.-D.; Lin, C.-S.; Zhang, W.-L.; Zhang, H.; He, Z.-Z. *Inorg. Chem.* **2011**, *50*, 5679−5686.
(14) Isaenko, L.; Vasilyeva, I.; Merkulov, A.; Yelisseyev, A.; Lobanov, S. *J. Cryst. Growth.* **2005**, *275*, 217−223.
(15) Chen, B.; Zhu, S.; Zhao, B.; Lei, Y.; Wu, X.; Yuan, Z.; He, Z. *J. Cryst. Growth.* **2008**, *310*, 635−638.
(16) Shevchuk, M. V.; Atuchin, V. V.; Kityk, A. V.; Fedorchuk, A. O.; Romanyuk, Y. E.; Calus, S.; Yurchenko, O. M.; Parasyuk, O. V. *J. Cryst. Growth.* **2011**, *318*, 708−712.
(17) Isaenko, L.; Yelisseyev, A.; Lobanov, S.; Titov, A.; Petrov, V.; Zondy, J.-J.; Krinitsin, P.; Merkulov, A.; Vedenyapin, V.; Smirnova, J. *Cryst. Res. Technol.* **2003**, *38*, 379−387.
(18) Rigaku. *CrystalClear*; Rigaku Corporation: Tokyo, Japan, 2008.
(19) Sheldrick, G. M. *Acta Crystallogr., Sect. A: Found. Crystallogr.* **2008**, *64*, 112−122.
(20) Brese, N. E.; Keeffe, M. O. *Acta Crystallogr., Sect. B: Struct. Sci.* **1991**, *47*, 192−197.
(21) Brown, I. D.; Altermatt, D. *Acta Crystallogr., Sect. B: Struct. Sci.* **1985**, *41*, 244−247.
(22) Gelato, L. M.; Parthé, E. *J. Appl. Crystallogr.* **1987**, *20*, 139−143.
(23) Kurtz, S. K.; Perry, T. T. *J. Appl. Phys.* **1968**, *39*, 3798−3813.
(24) Payne, M. C.; Teter, M. P.; Allan, D. C.; Arias, T. A.; Joannopoulos, J. D. *Rev. Mod. Phys.* **1992**, *64*, 1045−1097.
(25) Clark, S. J.; Segall, M. D.; Pickard, C. J.; Hasnip, P. J.; Probert, M. J.; Refson, K.; Payne, M. C. *Z. Kristallogr.* **2005**, *220*, 567−570.
(26) Rappe, A. M.; Rabe, K. M.; Kaxiras, E.; Joannopoulos, J. D. *Phys. Rev. B* **1990**, *41*, 1227−1230.
(27) Bellaiche, L.; Vanderbilt, D. *Phys. Rev. B* **2000**, *61*, 7877−7882.
(28) Lin, J. S.; Qtseish, A.; Payne, M. C.; Heine, V. *Phys. Rev. B* **1993**, *47*, 4174−4180.
(29) Kleinman, L.; Bylander, D. M. *Phys. Rev. Lett.* **1982**, *48*, 1425−1428.
(30) Monkhorst., H. J.; Pack, J. D. *Phys. Rev. B* **1976**, *13*, 5188−5192.
(31) Chen, C. T.; Lin, Z. S.; Wang, Z. Z. *Appl. Phys. B: Laser Opt.* **2005**, *80*, 1−25.
(32) Godby, R. W.; Schluter, M.; Sham, L. J. *Phys. Rev. B* **1988**, *37*, 10159−10175.
(33) Wang, C. S.; Klein, B. M. *Phys. Rev. B* **1981**, *24*, 3417−3429.
(34) Bera, T. K.; Jang, J. I.; Song, J.-H.; Malliakas, C. D.; Freeman, A. J.; Ketterson, J. B.; Kanatzidis, M. G. *J. Am. Chem. Soc.* **2010**, *132*, 3484−3495.
(35) Ma, H. W.; Guo, G. C.; Wang, M. S.; Zhou, G. W.; Lin, S. H.; Dong, Z. C.; Huang, J. S. *Inorg. Chem.* **2003**, *42*, 1366−1370.
(36) Assoud, A.; Soheilnia, N.; Kleinke, H. *Z. Naturforsch. Teil B.* **2004**, *59*, 975−979.
(37) Schevciw, O.; White, W. B. *Mater. Res. Bull.* **1983**, *18*, 1059−1068.